Check for updates

# Reviewing experimental studies on sensible thermal energy storage in cementitious composites: report of the RILEM TC 299-TES

**Juan J. Gaitero** · **Achutha Prabhu** · **Daniel Hochstein** · **Reza Mohammadi-Firouz** ·
**Claudiane Ouellet-Plamondon** · **Mathieu Bendouma** · **Didier Snoeck** · **Irene Ramón-Álvarez** ·
**Sergio Sánchez-Delgado** · **Manuel Torres-Carrasco** · **Jorge S. Dolado**

**Abstract** Thermal energy storage (TES) systems have been a subject of growing interest due to their potential to address the challenges of intermittent renewable energy sources. In this context, cementitious materials are emerging as a promising TES media because of their relative low cost, good thermal properties and ease of handling. This article presents a comprehensive review of studies exploring the use of cementitious materials, particularly concrete, as sensible heat storage media at varying scales, ranging from laboratory investigations to prototype evaluations. Starting from the different kinds of energy storage systems and applications where concrete has been used as a storage media, this article reviews the important properties which makes them a suitable material for the purpose. Reported observations are discussed and summarised based on concrete mix composition/design, aggregate/addition type, size gradation, etc., and performance of these materials. Finally, different cement-based prototypes are examined highlighting their strengths and weaknesses, and general conclusions are drawn.

**Keywords** Thermal energy storage · Sensible heat storage · Characterization techniques

rilem

# 1 Introduction

Sensible heat storage is the most common, simple, low-cost and longstanding method for storing energy [1]. In sensible heat storage systems, no phase change or chemical reaction occurs. The only effect of storing or releasing energy is the increase or decrease of the temperature of the storage medium [2]; put aside minor effects like thermal expansion. The storage medium is either available in solid (rocks, metals, concrete…) or liquid form (oil, water, molten salts…) [3, 4]. Apart from the cost, one of the main parameters for choosing the most appropriate medium is the range of working temperatures, which can vary from ambient temperature fluctuations in building walls to about 400–600 °C for high temperature storing systems [5]. Such temperature range does not only affect the amount of energy stored in the material but also its durability. Rapid thermal cycling over large temperature ranges can quickly degrade the materials due to the internal strains resulting from thermal expansion.

In this paper, we will describe the main systems that use concrete as sensible energy storage medium, the underlying theoretical background, the key techniques for the characterization of material properties and summarize the research outputs in the field.

# 2 Thermal energy storage (TES) systems

Sensible heat storage has been used for centuries in the building envelope to reduce the indoor temperature fluctuations derived from ambient temperature variations and to delay the air temperature minimum and maximum [6]. However, within the building sector, sensible energy storage can be used in several ways: to compensate for daily or even seasonal demand or to supply urban heating networks [7, 8]. In general, in the case of daily storage, the process is passive since the thermal energy of the system is delivered to its environment. In contrast, seasonal storage is generally active: the accumulated heat is conducted to a storage system and is delivered when needed. TES for building applications is generally low temperature. Heat storage can also be used to power industrial processes at medium/high temperature (100–200 °C) [9, 10] and at very high temperature (above 1000 °C) [10].

The valorisation of the stored sensible energy can also be applied in many fields such as the paper, textile and chemical industries [11, 12]. Waste heat recovery is mainly used for energy savings with absorption heat pumps [13]. When water is used as storage media, the temperature is generally limited to 100 °C due to ebullition. For higher temperatures, other low cost and effective materials should

———

*Present Address:*

J. J. Gaitero (✉)
Department of Physics, University of the Basque Country UPV/EHU, Barrio Sarriena s/n, 48940 Leioa, Spain
e-mail: juanjose.gaitero@ehu.eus

J. J. Gaitero · A. Prabhu
TECNALIA, Basque Research and Technology Alliance (BRTA), Astondo Bidea, Edificio 700, 48160 Derio, Spain

D. Hochstein
Department of Civil and Environmental Engineering, Manhattan College, 4513 Manhattan College Parkway, Riverdale, NY 10471, USA

R. Mohammadi-Firouz
Department of Civil Engineering, ISISE, University of Minho, Campus de Azurém, 4800-058 Guimarães, Portugal

C. Ouellet-Plamondon · M. Bendouma
Department of Construction Engineering, École de Technologie Supérieure, Université du Québec, 1100 Rue Notre-Dame Ouest, Montréal, Québec, Canada

D. Snoeck
BATir, Université Libre de Bruxelles (ULB), 50 Av F.D. Roosevelt, CP 194/02, 1050 Brussels, Belgium

I. Ramón-Álvarez · M. Torres-Carrasco
Materials Sciences and Engineering Department-IAAB, University Carlos III of Madrid, Avda. Universidad 30, 28911 Leganés, Madrid, Spain

S. Sánchez-Delgado
Thermal and Fluids Engineering Department, University Carlos III of Madrid, Avda. Universidad 30, 28911 Leganés, Madrid, Spain

J. S. Dolado
Centro de Física de Materiales, CSIC-UPV/EHU, Paseo Manuel de Lardizábal 5, 20018 Donostia-San Sebastián, Spain

be used [14]. Molten nitrate salts are often used in solar thermal plants, but their durability above 600 °C limit their application, which underlines the need to develop alternatives [15].

Finally, the storage of sensitive energy can also be used to produce electricity: heat can be converted into mechanical energy and electricity [16]. In addition to opening the way to an alternative to fossil fuels, it increases the production potential of solar thermal power plants [16].

# 3 Key properties for "sensible TES"

A good material for a TES-type application implies a low cost, a good thermal capacity ($\rho \cdot c_\mathrm{p}$), stability and durability under service temperatures [17]. The cumulated thermal energy within a certain mass of material $Q$ can be expressed as:

$$Q = \rho \cdot c_\mathrm{p} \cdot V \cdot \Delta T \tag{1}$$

where $\rho$ is the density [kg m$^{-3}$], $c_\mathrm{p}$ the specific heat capacity [J kg$^{-1}$ K$^{-1}$], V the volume [m$^3$] and $\Delta T$ the temperature difference [K]. Therefore, in this equation only $\rho$ and $c_\mathrm{p}$ are materials properties. In particular, the specific heat capacity is defined as the amount of energy [J] absorbed per unit mass [kg] of the material when its temperature increases one degree without any change of phase or chemical composition [18]. For the cementitious systems (concrete), $c_\mathrm{p}$ varies between 0.7 and 1.2 kJ kg$^{-1}$ K$^{-1}$ depending on the temperature and the specific composition of the composite. In Eq. (1), it is to be observed that the specific heat has a mean value within the exercise temperature range [17].

Similarly, the density indicates the mass concentration of an object in relation to the space it occupies and is commonly expressed in kg m$^{-3}$ or g cm$^{-3}$. The density of a solid also varies with the temperature and pressure, and depends on many factors, such as the porosity, chemical composition and crystalline structure. In the case of concretes for TES systems, the density varies typically from 2000 to 2500 kg m$^{-3}$.

The higher the volumetric heat capacity $\rho \cdot c_\mathrm{p}$, the lower the volume per thermal unit required. However, another fundamental parameter for sensible heat TES is the velocity at which thermal energy can be stored and recovered. Such a characteristic is a function of

the thermal diffusivity which is defined as the ratio of the transferred heat to the stored heat:

$$\lambda = \frac{\text{Transferred heat}}{\text{Stored heat}} = \frac{k}{\rho \cdot c_\mathrm{p}} \tag{2}$$

where $k$ is the thermal conductivity [W m$^{-1}$ K$^{-1}$] [17] and it is defined as the amount of energy transferred by a material per unit of time, thickness and temperature difference. Thermal conductivity is a temperature-dependent property that varies widely with composition and internal structure, with values as low as 0.08 W m$^{-1}$ K$^{-1}$ for polystyrene foamed concrete and 0.8–1.2 W m$^{-1}$ K$^{-1}$ for more regular unreinforced concretes and mortar [19–21].

The thermal expansion coefficient, cyclic stability linked to its service life, availability of the resources, cost and production methods are other important factors to be taken into consideration [22, 23].

The mechanical properties should, furthermore, show good stability, high fracture toughness and compressive strength [24]. The solution needs to be durable and sustainable [24]. There should not be any decomposition and the material should be chemically stable, non-toxic, non-explosive and compatible with other construction materials.

Cementitious materials have good stability, thermal capacity, diffusivity for thermal comfort regulation, high mechanical properties, durability and are chemically sound materials to use as thermal energy storage. Due to the ease of manufacturing, the overall base cost is limited, and any kind of shape is possible, linked to the formwork used.

The following section provides an overview of current methods employed in characterization of materials for thermal energy storage applications.

# 4 Current experimental test procedures and characterization techniques of TES materials

## 4.1 Thermal properties

### 4.1.1 Thermal conductivity

The Eurocode 2 includes recommendation for the thermal conductivity of concrete, $k_\mathrm{c}$, at different temperatures [25] because thermal conductivity is

influenced by many factors: moisture content, type and volume of the aggregates, water to cement ratio of cement paste, etc. [18]. This sensitivity could be extended in case of thermal conductivity determination of cement composites. Standardized methods exist for measurement of thermal conductivity of polymeric and insulation materials, however, there is a lack of standard methodology in case of TES materials. Several methods are addressed in the literature to determine the thermal conductivity of the materials, while each should be adopted with great care. In order to measure the thermal conductivity of TES materials, measurement condition, type of the material, sample size and the energy storing technology (sensible, latent, or thermochemical heat) should be considered in selecting the proper method [26].

In principle, there are two kinds of thermal conductivity determination methods: (1) steady-state techniques, which are not a function of time and the temperature at each point of the sample is constant; (2) transient approaches, which are based on the simultaneous determination of heat flux and heat capacity [27].

The steady-state methods include Guarded Hot Plate (GHP) method, heat flow meters (HFM), comparative method, direct heating (Kohlrausch) method, and pipes and hot wire method. From the known transient methods, transient hot wire/hot strip, transient plane source (TPS) method, laser flash analysis technique, temperature modulated DSC (TM-DSC), 3ω method, thermocouple method and photo thermal methods could be named. In this section, the details of the most popular methods for evaluating the thermal conductivity of TES materials, in steady and non-steady states, are briefly described.

*4.1.1.1 Steady-state: guarded hot plate (GHP)*  The GHP is a popular and reliable method for the determination of the thermal conductivity of glasses, ceramics, polymers and thermal insulation materials. [28, 29]. GHP setup (shown in Fig. 1) consists of one or two parallel cold plates (or cylinders), electrically heated inner plate and thermal insulation to make sure that the generated heat only passes through the sample [27]. The thermal conductivity can be calculated when the system reaches the steady-state, based on the Fourier's conduction equation [26]:

$$k_c = (Q \cdot d)/(2A \cdot \Delta T) \qquad (3)$$

where $Q$ is the total input into the hot plate, $d$ is the averaged sample thickness, $A$ is the measurement area and $\Delta T$ is the mean temperature difference. Commercial devices perform this test from $-160$ to 700 °C for materials with relatively low thermal conductivity of up to 2 W m$^{-1}$ K$^{-1}$. The GHP method is described in, e.g., ISO 8302, ASTM C177 or DIN EN 12667.

*4.1.1.2 Steady-state: heat flow meter (HFM)*  The HFM is another accurate technique to test materials with low thermal conductivity (up to 2 W m$^{-1}$ K$^{-1}$) in the temperature range $-20$ to 100 °C [26]. The overall
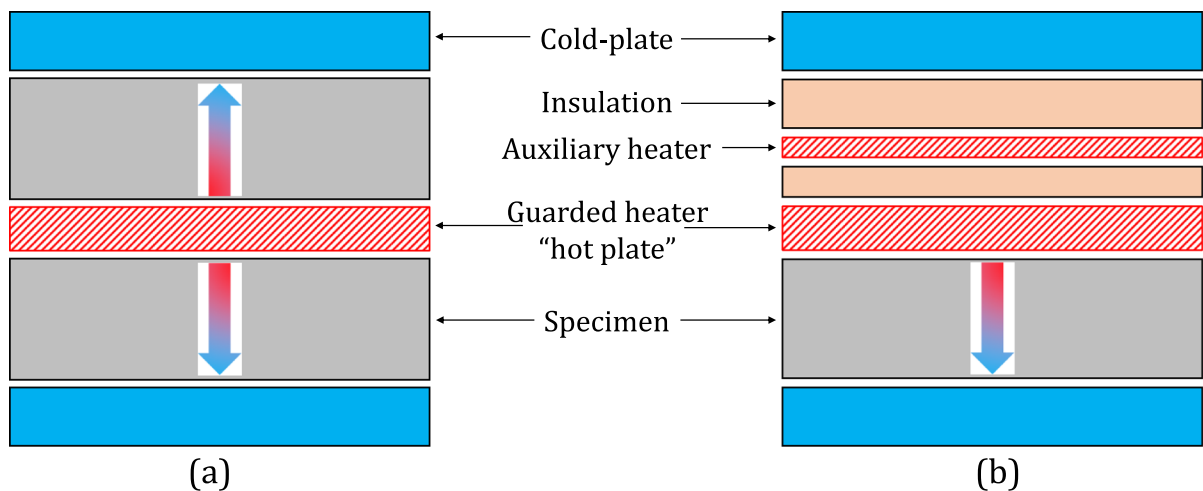


**Fig. 1** Principle of the guarded hot plate method: **a** two-specimen apparatus, **b** single-specimen apparatus

setup configuration (see Fig. 2) is similar to the GHP system; however, it uses transducers to measure the heat flux density through the sample. Then, the heat flux registered throughout the test is used for calculating of the thermal conductivity, according to the Fourier's law [26]. However, the number of available research data using this method is scarce in the literature [30, 31].

The measurement of the thermal conductivity by means of the HFM method is based on ASTM C518, ASTM C1784, ISO 8301, JIS A1412, DIN EN 12664 and DIN EN 12667 standards.

*4.1.1.3 Transient: transient hot wire/hot strip (THW)* THW method is the most common thermal conductivity measurement tool for electrically non-conductive solids, liquids and gases. It is faster than steady-state techniques and can be applied in a wider range of temperature and thermal conductivity ratios. The experimental setup consists of a thin electrically resistive wire placed in the centre of the sample (see Fig. 3). Thermocouples are also placed in the sample at different distances from the central thin wire. When a known electrical current is passed through the wire, it heats up due to the Joule effect. By measuring the temperature variations as a function of time at different points, a temperature profile can be obtained. From this temperature profile and using heat transfer theory, it is possible to calculate the thermal conductivity of the material [26].



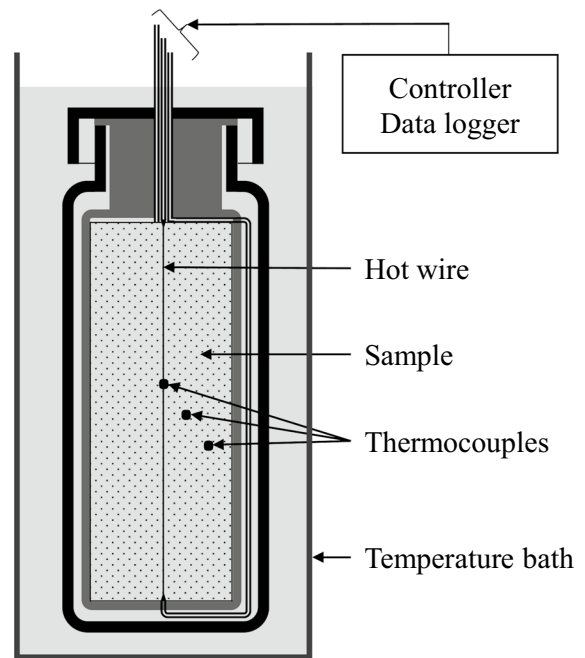**Fig. 3** Scheme of THW technique

The main drawbacks of THW method are the complexity of the setup and the dependency of the accuracy in factors like hot wire shape and location, material uniformity, measurement duration and environmental conditions [26]. Therefore, proper calibration and consideration of all the variables are key for obtaining accurate results.
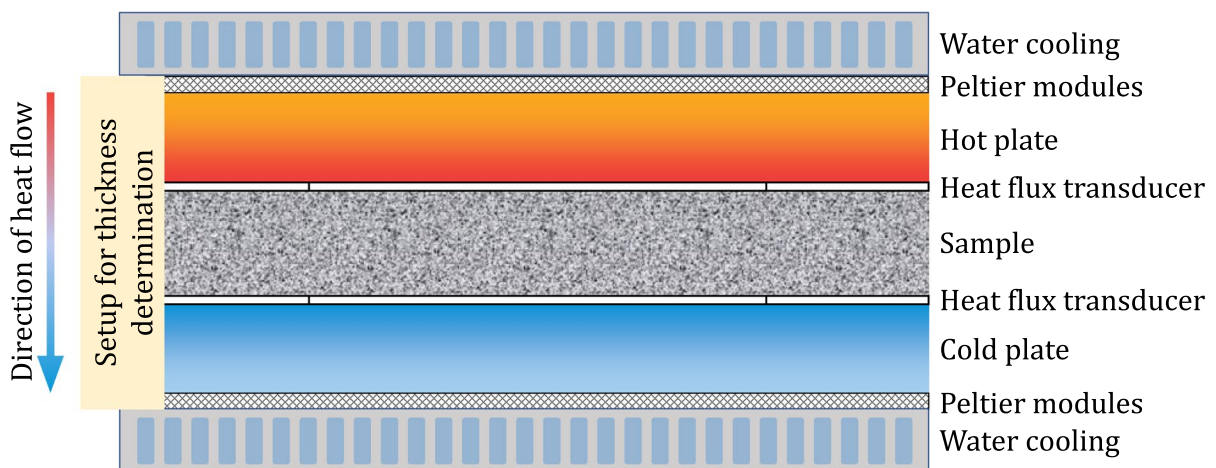


**Fig. 2** Schematic of a heat flow meter

*4.1.1.4 Transient: transient plane source (TPS)* TPS technique can be used for measuring solid (including powder) and liquid samples with thermal conductivities from 0.001 to 1800 W m$^{-1}$ K$^{-1}$ in the temperature ranges from $-35$ °C to 750–1000 °C (oxygen free) [26]. The wide testing range makes it the most frequent technique to determine the thermal conductivity of TES material [32].

TPS method uses a circular double spiral of nickel covered material as sensor and heat generator [33]. The sensor is placed between two identical specimens of the material to be studied (see Fig. 4) [26] and a constant electric current is passed through the spiral. The heat generated by the current is partially transferred to the studied material. However, it also rises the temperature and, thus, increases the resistance of the spiral. At constant electric current, the voltage in the coil is proportional to electric resistance of the coil. Therefore, with knowledge of the voltage variation with time, it is possible to calculate the thermal conductivity and volumetric heat capacity of the material by means of the Fourier's law [34].

As in the case of the Transient Hot Wire technique, it is important to consider that the accuracy of the measurement can be affected by factors such as the geometry and thermal properties of the sensors, the homogeneity of the sample and the environmental conditions. Therefore, it is essential to perform proper calibrations and consider these variables in order to obtain accurate results using the Transient Plane Source technique.

### 4.1.2 Heat capacity

Generally, there are two techniques to determine the heat capacity of a solid: Differential Scanning Calorimetry (DSC) and Drop Method (DM) [35]. In DSC, a constant heat flow can be applied to counterbalance the heat content with the heating/cooling process and the heat capacity can be obtained by integrating the heat flow changes. However, in DM, the studied sample and the reference sample are placed in the sample holder at room temperature to drop them directly into a calorimeter held at a higher temperature. The calorimeter measures the heat flow evolution while the sample heats to the temperature of the calorimeter. DM was reported to be increasingly important due to its high precision calorimetric data at up to 2700 °C owing to its special 3D heat sensor [35, 36]. However, due to the availability and wide usage of DSC techniques in TES field, it will be the focus in this section.

As stated above, the most used technique to determine the specific heat capacity is DSC. It is a thermoanalytical technique in which the difference in the amount of heat required to increase the temperature of a sample and reference is measured as a function of temperature. Basically, two methods of DSC are commonly used: (1) the power-compensation DSC and (2) the heat-flux DSC (see Fig. 5). The difference between them lies in design and measuring principle. However, the characteristic feature of all DSC measurement systems is the twin-type design and the direct indifference connection of the two-measuring system. In power-compensation DSC technique, the temperatures of the sample and the reference are made identical by varying the power input to the two furnaces; the energy required to do this is a measure of enthalpy or heat capacity changes in the sample relative to the reference. In heat-flux DSC systems, a low resistance heat flow path connects the sample and the reference, while the assembly is enclosed in a furnace. The enthalpy or heat capacity change in a sample causes a difference in its temperature relative to the reference [37].

For both methods (power-compensation and heat-flux), the sample size is a key parameter that typically



**Fig. 4** Scheme of transient plane source technique
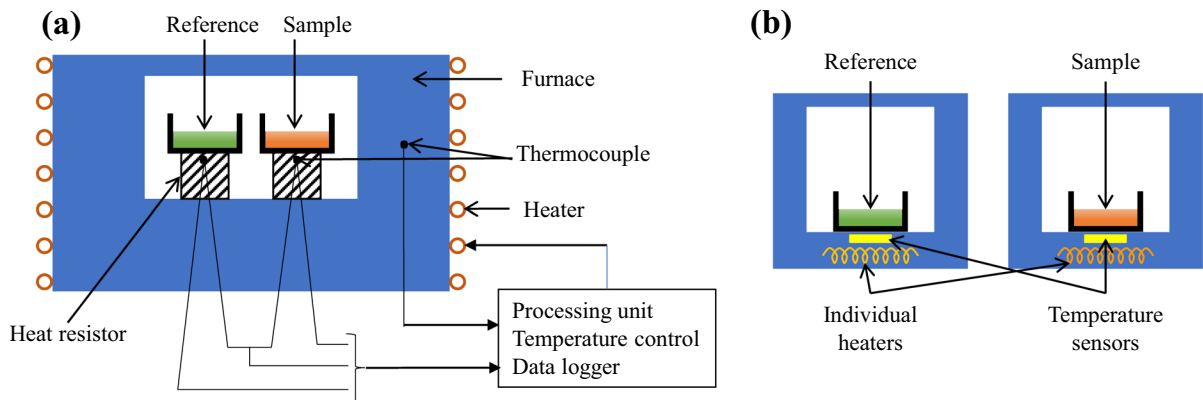
Sample

TPS sensor
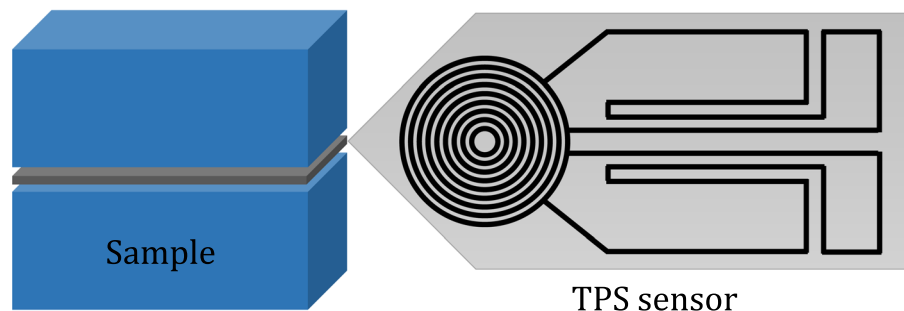
**Fig. 5** Scheme of DSC techniques: **a** heat-flux method and **b** power-compensation method

falls within the range of a few milligrams to several tens of milligrams. It is worth mentioning that this parameter has a high impact on the sensitivity and accuracy of the measurements. For small sample sizes, the signal-to-noise ratio may be low. However, if the sample size is excessively large, heat transfer can be slower, resulting in longer equilibration times.

Prior to the heat-flux DSC test, it is important to make the calibration for all reference materials for melting point, enthalpy and heat capacity. Different reference materials can be used based on the testing equipment, but most of them are metals and among them, indium is quite popular. As mentioned earlier, a calorimeter can supply heat to the sample by electrical or thermal resistance [38]. In heat flux DSC, the heat is supplied to the sample through a thermal resistance. Therefore, the heating mode or the temperature program, is another important factor. Several temperature programs are reported in literature, however, the most popular ones for measuring TES materials are the dynamic method, the iso-step method and the areas method [39].

### 4.2 Microstructure and composition (chemical and mineralogical)

Although thermal properties are the primary properties to be considered when using a material as a TES, there are other complementary characterisations that help to understand and predict the behaviour of materials. There are numerous techniques for cementitious materials characterization [40]. Focusing on solar thermal storage applications, it should be noted that

techniques such as X-ray diffraction [41–45], thermogravimetric analysis (DTA-TGA) [27, 46–49], helium pycnometry [50, 51], gas absorption and mercury porosimetry [52–55], BSEM/EDX [56–60] and Confocal Raman Microscopy (CRM) [61, 62] can provide very valuable information to explain the behaviour of the systems. Nevertheless, no further information will be provided in this document because they are standard techniques widely used in materials science.

### 4.3 Durability assessment

One of the main challenges for TES systems is the durability of the storage materials under thermal cycling and hence it is important to design reliable tests to predict it. Here, three parameters come into play: temperature range, heating and cooling rates and number of cycles.

The main negative effects of the exposure of concrete to high temperatures are the differential thermal expansion of its constituent phases and their decomposition or transformation into other polymorphs. These effects may lead to the generation of thermal stresses within the material due to volumetric changes, or the release and accumulation of gases [89]. Such stresses increase the likelihood of cracking and/or spalling, especially at high heating and cooling rates and as the number of thermal cycles increases [63–66].

For slow heating rates, residual compressive strength of concrete after heating to high temperatures can be divided into three main stages: (1) from the room temperature to 300 °C, where compressive

strength remains constant or even increases slightly; (2) from 300 to 800 °C, where compressive strength decreases drastically; and (3) 800 °C onwards, where almost all the compressive strength is lost [67]. The residual tests are generally done using electric furnace for high temperature exposure and the heating process is commonly started with a determined heating rate until reaching the target temperature, followed by an isothermal part for a specific duration of time and a cooling ramp. Emerson et al. [89] selected the heating rate of 9 °C min$^{-1}$ and 300 °C and 500 °C isothermal period of 2 h, based on their previous research [90]. They exposed high performance concrete to high temperatures for 10 thermal cycles and performed the residual compressive tests after each cycle. Roig-Flores et al. [72] used a heating rate of 1 °C min$^{-1}$ for the low-speed cycle for the dehydration stage followed by an 8 °C min$^{-1}$ for the thermal cycles to evaluate residual compressive strength of concrete with calcium aluminate cement for energy storage. Fernandez et al. [64] also reported a review of mechanical characterization (compressive and flexural strength) on five different concrete mixes as sensible TES media, incorporating various materials such as Portland cement, calcium aluminate cement, fly ash, metallic and polypropylene (PP) fibres. They compared the residual compressive tests of these mixtures after 25–30 thermal cycles of 500–600 °C. By contrast, Zeng et al. [68] chose a much lower temperature range of 5 45 °C and a much higher number of cycles (100, 500, and 1000) to evaluate the effect of thermal cycling fatigue on the mechanical properties and microstructure of cement pastes. Finally, several existing test methods on moisture migration and water pooling in concrete spalling are reported by Kannangara et al. [65].

### 4.4 Determination of costs and environmental impacts

The selection of TES materials, in addition to their thermal, physicochemical and mechanical properties, is influenced by economic and environmental factors. However, there is no standard methodology for the determination of the costs and environmental footprint of each solution. For example, Batuecas et al. [69] showed that indicators, like Global Warming Potential (GWP) or Available Water Remaining (AWARE), can be calculated using as a functional unit the dosage per m$^3$ of mortar or concrete, although other authors [70] suggest that for this application it would be preferable to do it per unit of stored energy in order to indicate the performance of a solar thermal installation. In the same line, Khare et al. [24] used a selection software package, EcoAudit (a CES tool from Granata Design), to identify suitable SHS materials for high temperature (above 500 °C) TES systems, taking into account the cost and environmental credentials of the materials [24]. Alternatively, Laing et al. [71] observed by life cycle analysis (LCA) that the replacement of the two-tank molten salt storage system of a real solar thermal power plant by a hypothetical concrete storage system had advantages concerning environmental and economic impacts [71]. Miro et al. [72] studied the environmental impact of high temperature TES systems based on molten salts and concrete by calculating their embodied energy using the cumulative energy demand (CED) method in combination with the data from EcoInvent materials database [73].

Authors like Emerson et al. [75] only considered technical and economic aspects, reporting that concrete bricks can potentially replace aggregates as a TES medium for thermocline solar energy storage systems. Similarly, Selvam et al. [73] included production costs as one of the parameters to consider for the development of concrete mixtures for TES in solar power generation. Finally, Fernandez et al. [23] used the methodology for materials selection developed by Prof. Ashby [74, 75] to give an overview of materials suitable to be used for SHS at temperatures between 150 °C and 200 °C. Two different scenarios were considered: long term and short term SHS. Although the proposed methodology allows combining multiple objectives and restrictions of use, this case study focused on minimizing the costs.

## 5  Available data/results

The performance of a concrete mixture with respect to its ability as a SHS material depends on many factors, including, the type of cement binder, types and properties of the aggregate, water-cementitious material ratio, porosity including entrained air, the addition of fibre reinforcement and the inclusion of other materials. The properties that have been used to assess concrete's effectiveness as a SHS material

include residual compressive strength, thermal conductivity, specific heat, coefficient of thermal expansion, shrinkage and unit cost.

### 5.1 Effect of cement type

The two types of cement most commonly studied are Portland cement (PC) and calcium aluminate cement (CAC). CAC, which was initially developed for use as a sulphate resistant cement, is commonly used for refractory concrete and is able to withstand high temperatures (up to 600 °C) that SHS concrete is exposed to, in energy storage devices.

The hydration of PC produces mainly calcium silicate hydrate gel (C–S–H) and calcium hydroxide (CH), although hydrated aluminate, ferrite and sulphate phases are often present in smaller proportions [42]. Different authors have described the reactions that occur with an increase of temperature in PC matrix [44, 60, 76]. It is generally accepted that evaporable water (free and physically bound water) is not present at temperatures over about 105 °C, although some authors increase such upper limit to 120 °C. Decomposition of the C–S–H gel, carboaluminate hydrates, ettringite and CH takes place progressively between 100 °C and 600 °C. In all cases, the release of gaseous water can lead to a build-up of pressure that can severely damage the material. Water vapor trapped in the matrix can also react with unhydrated cement grains by the so-called internal autoclaving [45]. The dehydration of C–S–H and CH leads to the formation of CaO (calcium oxide), which may rehydrate upon cooling resulting in swelling. Nevertheless, if the PC is blended with certain supplementary cementitious materials or pozzolans, this risk decreases due to the larger amount of C–S–H produced relative to CH [5].

The hydration of CAC mainly produces the calcium aluminate hydrates $CAH_{10}$ and $C_2AH_8$. $CAH_{10}$ is mainly produced when the temperature is below 20 °C, $C_2AH_8$ and aluminium hydroxide ($AH_3$) are produced when the hydration temperature is around 30 °C and $C_3AH_6$ and $AH_3$ are the hydration products when the temperature is above 55 °C [77]. Additionally, over time $CAH_{10}$ and $C_2AH_8$ are only metastable and convert to $C_3AH_6$ and $AH_3$ [78]. Since the hydrate $C_3AH_6$ is denser than $CAH_{10}$, the overall cement paste is less dense and contains more pores. To prevent this evolution, supplementary cementitious materials high in silica are added which retard this transformation by forming more stable calcium aluminates containing silica (siliceous hydrogarnet phases or strätlingite).

Ukrainczyk and Matusinović [77] demonstrated that the thermal properties of CAC pastes vary with hydration temperature. It was observed that the thermal diffusivity decreases with hydration when CAC is cured at 15 °C, while it increases with hydration when the temperature is increased to 30 °C. Both the thermal diffusivity and thermal conductivity increased with a decrease in the water-cement ratio (11% and 8% increase, respectively between water-cement ratios of 0.4 and 0.3). Also, the thermal diffusivity decreased slightly as the temperature was raised (between 10 and 80 °C) while the thermal conductivity increased within the same temperature range.

Dos Santos [79] measured the thermal properties of CAC concretes with the same water-cement ratio, but containing different aggregate grain size distribution. Dos Santos first measured the thermal conductivity, thermal diffusivity and specific heat as a function of temperature from room temperature to 1000 °C at 100 °C intervals. Then, specimens were heated to 1000 °C, held there for 6 h and the measurements were repeated following the same procedure. During the initial heating, all three properties went through the same evolution of initially increasing (region 1—loss of absorbed water), then decreasing (region 2—loss of water from hydrated phases) and once again increasing (region 3—densification/sintering) as the temperature was raised. This contrasts with the tendency observed by Pan et al. [80] on the specific heat of a PC concrete containing fly ash and granite aggregate between 100 °C and 600 °C. The results plotted in Fig. 6 show that specific heat increased very fast up to 300 °C and followed a slow linear increase from 300 °C to 600 °C. Nevertheless, during the second heating, the thermal conductivity and specific heat of CAC concretes [79] also increased as the temperature increased, with a significant change in the specific heat. On the contrary, the thermal diffusivity decreased until a temperature of approximately 700 °C and then slightly increased.

John et al. [5] reported that the type and amount of cementitious materials of PC and CAC concretes with silica fume and fly ash had little impact on thermal conductivity or specific heat.
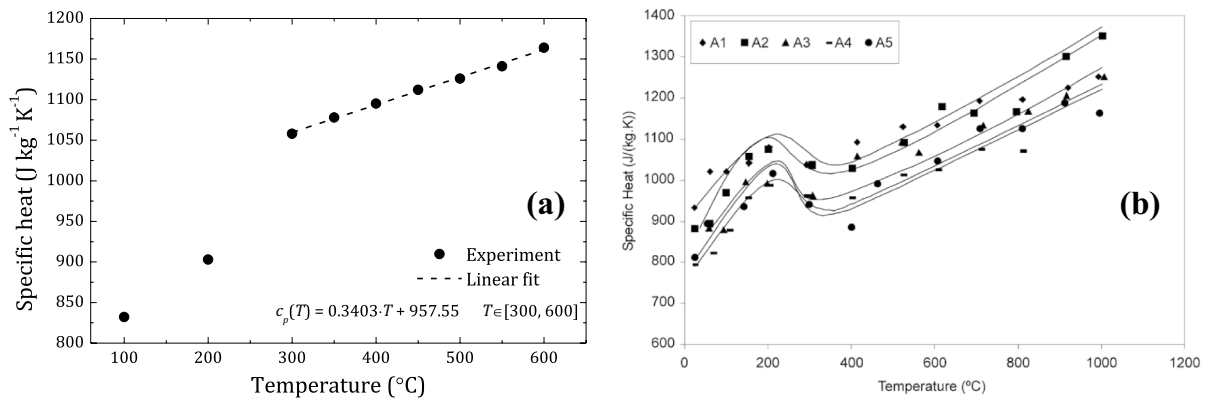
**Fig. 6 a** Specific heat at elevated temperatures and linear fit to the data in the range 300–600 °C for PC concrete. Data adapted from [80]. **b** Specific heat as a function of temperature for different CAC concrete mixes during the first heating. Image taken from [79]

John et al. [63] demonstrated the superior properties of CAC concrete with respect to PC concrete. All the mixes contained only fine aggregate and both steel and PP fibres. The PC mixes also contained either fly ash or a mixture of fly ash and silica fume. The concrete specimens were initially heated to 500 °C and held there for 2 h until they were returned to room temperature. The thermal fatigue cycles involved raising the temperature to 300 °C where it was held for 2 h, raising it further to 500 °C where it was held for another 2 h and then returning the temperature to ambient conditions. All specimens were exposed to 10 thermal fatigue cycles. The compressive strength was measured before the thermal cycling began and at the end of each cycle. It was observed that all of the reduction in compressive strength occurred within the first 3 cycles. PC concretes retained at least 50% of their initial compressive strength while in CAC concretes this value increased to over 75%. Unfortunately, the estimated cost of CAC concretes ($600 m$^{-3}$) was much higher than PC concretes ($120–140 m$^{-3}$).

Alonso et al. [78] observed a 50% decrease in the compressive strength of CAC mortar specimens exposed to a temperature of 550 °C for 8 h due to the dehydration of the cement paste. To prevent spalling, they pre-dried the samples at a temperature of 105 °C for 3 h and used a heating/cooling rate of 1 °C min$^{-1}$.

Although PC and CAC are the most studied cementitious materials, alkali activated cements (AAC) also present suitable properties for TES systems [81]. AACs are based on aluminosilicate precursors (such as kaolinite, fly ash and blast-furnace slag), activated by alkaline solutions. The most important factor to consider is the content of silicon and aluminium, but the alkaline activator and curing conditions have also an important impact on the final properties [82–84]. For example, in absence of Ca, the main phase of sodium AAC matrix is sodium-aluminosilicate-gel (N–A–S–H), which is stable up to 700–800 °C [85–87]. On the contrary, when this is not the case, Ca displaces Na in the surface of N–A–S–H by ion exchange to form C–(N)–A–S–H gel, whose dehydration and/or dehydroxylation starts at 100 °C. Nevertheless, the crystallization of phases like anorthite or gehlenite above 600 °C, give the material good mechanical and thermal properties [70, 81, 85, 88].

Finally, hybrid cements (HCs) containing 20–30 wt% of PC and 70–80 wt% of aluminosilicate precursors have also been studied [70, 81, 89, 90]. HCs usually contain soft alkaline salts in solid form to improve the mechanical properties at an early age [90]. Compressive strength of HC mortar samples after exposure to 500 °C was similar to that of the PC reference. On the contrary, thermal conductivities and specific heat of HC and AAC composites were higher compared to PC composites, allowing them to store more energy in a smaller volume and faster charge and discharge of the system (Table 1) [70].

## 5.2 Effect of water-cement ratio

The thermal conductivity of dry cement paste was measured by Hochstein and Meyer [91] at room

**Table 1** Specific heat and mass of material required to store 1 MJ of energy in a Portland cement mortar (PC 100 S), two alkali activated mortars (SLAG 100 S and SLAG 75 S 2–5 GW) and a hybrid cement mortar (HSLAG 5% 100 S) [70]

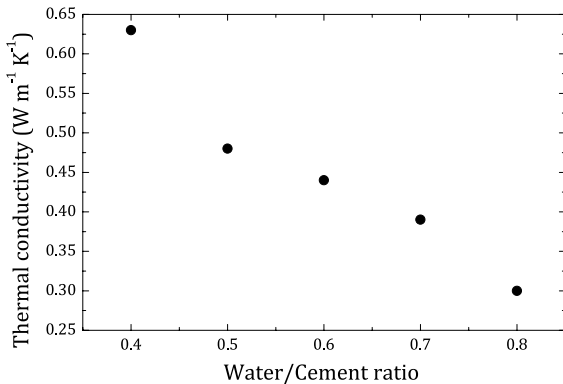| System | $C_p$ (J kg$^{-1}$ °C) | m (kg) |
|---|---|---|
| PC 100 S | 1710 | 5.85 |
| SLAG 100 S | 1602 | 6.24 |
| SLAG 75 S–25 GW | 1867 | 5.36 |
| HSLAG 5% 100 S | 1861 | 5.37 |



**Fig. 7** Thermal conductivity of cement paste [91]

temperature for water-cement ratios between 0.4 and 0.8. The thermal conductivity decreased as the water-cement ratio was increased, with a value of 0.63 W m$^{-1}$ K$^{-1}$ at 0.4 and a value of 0.33 W m$^{-1}$ K$^{-1}$ at 0.8 (Fig. 7). This decrease is caused by the increase in porosity as the water-cement ratio is increased. The thermal conductivity of concrete will be generally higher than that of cement paste since typical aggregate has a larger thermal conductivity than the cement paste. Zhang et al. [92] measured the thermal conductivity of concrete with both limestone and granite coarse aggregates. They recorded a drop from a thermal conductivity of approximately 2 W m$^{-1}$ K$^{-1}$ at a water–cement ratio of 0.3 to a value of approximately 1.4 W m$^{-1}$ K$^{-1}$ at a water–cement ratio of 0.6.

### 5.3 Effect of aggregate

The type and size of the aggregates used not only affects the thermal properties of SHS concrete, but perhaps more importantly, affects the durability of the concrete with respect to thermal cycling. The dissimilar values of the thermal expansion coefficients between the aggregate and cement paste can lead to thermal cracking as the concrete experiences its first thermal cycle and also later ones. Aggregates with high thermal expansion coefficients should be used in limited quantities.

Alonso et al. [78] studied the effect of thermal cycles on CAC mortar and concrete. The maximum aggregate sizes for the mortar and concrete mixes were 4 mm and 12 mm, respectively and were exposed to 8 and 75 thermal cycles respectively, between 290 °C and 550 °C. Both specimens experienced approximately 50% drop in compressive strength after the first cycle due to the dehydration of the matrix. However, while the strength of concrete specimens continued to decrease during subsequent thermal cycles, it appeared to stabilize in the mortars. The thermal fatigue, observed only in concrete specimens, is due to thermal mismatch between the matrix and the aggregates. Additionally, an increase in the number of thermal cycles was correlated with a decrease in the ultrasonic pulse velocity and an increase in pore sizes in the 10 μm range.

John et al. [5] observed a large reduction in the compressive strength for PC and CAC concretes compared to mortars, after 30 thermal cycles between 300 and 600 °C. However, the use of coarse aggregates also resulted in larger values of thermal conductivity and specific heat. This was attributed to the fact that the aggregate had both a higher thermal conductivity and specific heat than cement paste and specimens with coarse aggregate contained a larger proportion of aggregate by weight of binder. Besides, concretes had a larger unit weight than mortars which also increased thermal conductivity [93]. Dos Santos [79] also reported the significant effect of aggregate gradation on thermal conductivity than on specific heat for CAC concretes.

Roig-Flores et al. [56, 64] studied the effect of thermal cycling on CAC concretes with four types of aggregates: crushed basalt, synthetic clinker (CAT) from calcium aluminate cement, waste slag with a high iron salt content and siliceous aggregate. After one thermal cycle to 550 °C, the mix with the siliceous aggregate performed the worst, with a decrease in compressive strength of 74%. This is due to the high thermal expansion coefficient of silicious aggregates ($10.3 \times 10^{-6}$ °C$^{-1}$) that is almost double that of basalt ($6.4 \times 10^{-6}$ °C$^{-1}$). Additionally, the quartz in siliceous aggregate undergoes a transformation from

α-quartz to β-quartz between 500 °C and 650 °C, which results in a reversible expansion of 1.0–1.4%. During thermal fatigue tests conducted between 290 and 550 °C, cracks formed on the interface between the aggregate and cement paste due to the shrinkage of the paste and thermal expansion of the aggregate. Thermal conductivity was also reduced along thermal cycles. The highest reduction (30–35%) took place during the pre-conditioning of the samples at 105 °C due to the loss of evaporable water. Dehydration of the matrix during the first cycle results in an additional 18–30% reduction, while subsequent cycles only produce a cumulative drop of 7–12%. Comparison as a function of the type of aggregate, Table 2, shows that the concrete with silicious aggregates has a much higher thermal conductivity for temperatures

up to 300 °C and becomes similar to concrete with basalt aggregate at higher temperatures.

Kodur and Sultan [94] proposed a set of equations that predicts the thermal conductivity of high-strength concrete as a function of temperature from 0 to 1000 °C as shown in Fig. 8.

For siliceous aggregate:

$$k(T) = 2.00 - 0.0011T \quad T \in [0, 1000] \tag{4}$$

For carbonate aggregate:

$$k(T) = 2.00 - 0.0013T \quad T \in [0, 300] \tag{5}$$

$$k(T) = 2.21 - 0.0020T \quad T \in [300, 1000] \tag{6}$$

Girardi et al. [57] studied the effect of replacing natural aggregate (porphyry gravel and limestone

**Table 2** Thermal conductivity (W m$^{-1}$ K$^{-1}$) of concrete with various aggregate [64]

| Temperature (°C) | Aggregate | | | | |
|---|---|---|---|---|---|
| | Siliceous sand | Basalt | Ternary blend (basalt, CAT, slag) | Calcareous | CAT |
| 100 | 1.96 | 1.32 | 1.23 | 1.11 | 1.18 |
| 200 | 2.08 | 1.34 | 1.15 | 1.23 | 1.35 |
| 300 | 2.23 | 1.36 | 1.12 | 1.23 | 1.03 |
| 400 | 1.34 | 1.28 | 1.04 | 1.09 | 0.92 |
| 500 | 1.20 | 0.97 | 0.96 | 1.04 | 1.03 |
| 600 | 1.30 | 1.45 | 0.99 | 0.86 | 1.06 |

**Fig. 8** Thermal conductivity of concrete at elevated temperatures, as predicted by Kodur et al. [94]
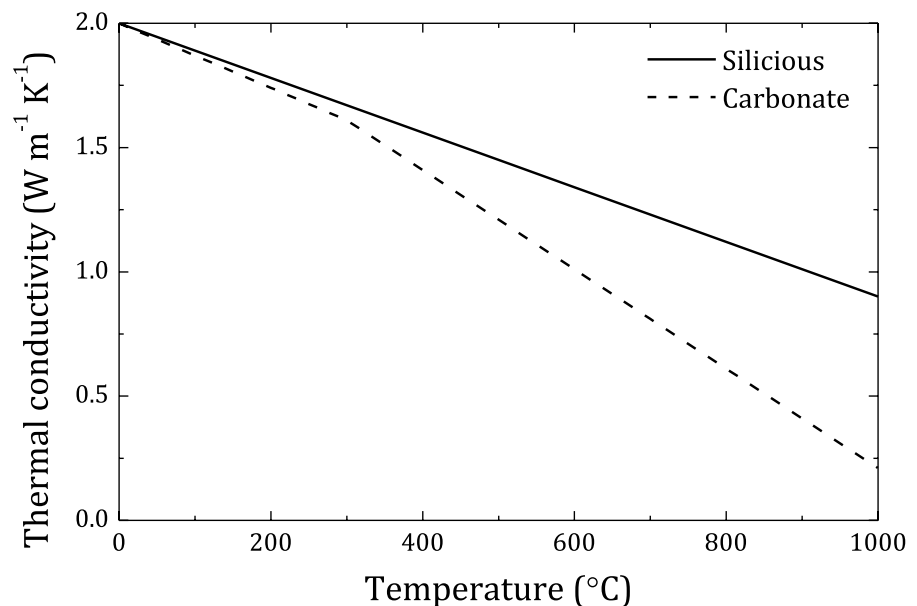
sand) in PC concrete with crushed recycled aggregate (CRA) made from concrete blocks. On thermal conditioning (at 150, 300 and 450 °C), the mixes with CRA experienced a larger mass loss at 4 h (about 6.0–6.5%) compared to mixes without CRA (approximately 5%). This was attributed to the moisture from cement paste residues contained in the CRA. The increased porosity of the CRA allowed the vapor to escape without an increase of pressure and hence no spalling was observed. Also, the specimens with CRA showed an increase in thermal conductivity and a minimal decrease of thermal conductivity on thermal conditioning at 300 °C compared to specimens with natural aggregates (Table 3).

### 5.4 Effect of polymeric fibres

Several authors [56] have added short PP fibres to the mix to decrease the tendency of concrete to spall at high temperatures. The voids leftover from the vaporization of the PP fibres at 350 °C help relieve stress as steam created at high temperatures can escape through these channels.

John et al. [75] demonstrated that PP fibres can prevent explosive spalling for high-strength PC concrete. High-strength concrete specimens with a water-cementitious material ratio between 0.15 and 0.30 were exposed to high temperatures using different heating rates including: 3, 5, 7 and 9 °C min$^{-1}$. For all the heating rates, the specimens that without PP fibres underwent explosive spalling at temperatures between 394 °C and 500 °C, while the specimens with 2 kg m$^{-3}$ of PP fibres were able to withstand a temperature of 600 °C. However, fibre-free specimens were found to perform better at higher heating rates due to the generation of a greater number of microcracks, which allowed the escape of water vapour.

Girardi et al. [57] had conflicting results concerning the effect of PP fibres on the thermal conductivity (see Table 3). The thermal conductivity and the coefficient of specific permeability was measured at 25 °C both before and after thermal conditioning at 300 °C for 4 h. For mixes that contained natural aggregate, the PP fibres caused an increase in the thermal conductivity. However, when the natural aggregate was replaced by CRA from concrete blocks, the addition of PP fibres caused a decrease in the thermal conductivity. These results show that the melting of PP fibres after they are exposed to elevated temperatures increases the permeability of the concrete and allows high-pressure vapor to escape and prevents spalling.

Ozger et al. [95] added polyamide fibres recycled from post-consumer carpets to concrete. During the first DSC scan, both fibre reinforced concrete (FRC) and reference (fibre-free) developed a peak at 100 °C as a result of the evaporation of absorbed moisture, which were not present during the second scan. Additionally, it was observed that at higher temperatures, the specific heat for the FRC decreased between the first and second scan due to the evaporation of the polyamide fibres. Overall, during the second scan, the specific heat of the FRC slightly decreased as the temperature increased. During the second scan the specific heat of FRC and conventional concrete were 0.63 J g$^{-1}$ K$^{-1}$ and 0.81 J kg$^{-1}$ K$^{-1}$, respectively, at 300 °C. For FRC and conventional concrete, the thermal conductivity at room temperature was found to be 1.30 W m$^{-1}$ K$^{-1}$ and 1.12 W m$^{-1}$ K$^{-1}$ respectively and at 300 °C, 1.16 W m$^{-1}$ K$^{-1}$ and 1.02 W m$^{-1}$ K$^{-1}$. At temperatures below 300 °C, the FRC displayed less thermal expansion than the control mix since the vapour could evaporate through the hollow fibre channels and showed good thermal stability up to 450 °C with no spalling.

**Table 3** Thermal conductivity and coefficient of specific permeability with CRA and PP fibres [57]

| Mix | Thermal conductivity (W m$^{-1}$ K$^{-1}$) | | Coefficient of specific permeability ($10^{-16}$ m$^2$) | |
| --- | --- | --- | --- | --- |
| | Before thermal conditioning | After thermal conditioning | Before thermal conditioning | After thermal conditioning |
| Natural aggregate | 0.74 | 0.53 | 2.0 | 139 |
| Natural aggregate and PP fibres | 0.89 | 0.81 | 40.0 | 872 |
| CRA | 1.03 | 1.01 | 20.6 | 325 |
| CRA and PP fibres | 0.92 | 0.91 | 7.5 | 773 |

## 5.5 Effect of nanoparticles

Jiang et al. [96] studied the effect of replacing 1% of cement by weight of cement by nanoparticles of silica (NS), magnesia (NM) and zirconia (NZ) on the thermal properties of CAC pastes. The specimens were conditioned by drying at 105 °C or fired at either 350 °C or 900 °C. For all pastes, the compressive strength, thermal conductivity and heat capacity decreased as the conditioning temperature was increased due to dehydration and increase in porosity. Nanoparticles tend to accelerate the hydration process by providing nucleation sites and promote a denser structure. The tested nanoparticles demonstrated notable improvement in the compressive strength relative to pure CAC paste at different conditioning temperatures. NZ had the largest increase at 105 °C, NS at 350 °C and NM at 900 °C. All of the nanoparticles increased the compressive strength when the conditioning temperature was either 105 °C or 350 °C, while NM showed a significant increase at 900 °C (NS and NZ showed minor decreases in strength). Specimens showed an increase in the thermal conductivity at conditioning temperatures of 350 °C and 900 °C, with NS and NM having similar values at 350 °C and NS having a higher value at 900 °C. NM had the most pronounced effect on the heat capacity with it causing an increase in specific heat for all conditioning temperatures. At temperatures above 400 °C the nanoparticles caused a significant increase in the coefficient of thermal expansion with approximate values of $6.5 \times 10^{-6}$ °C$^{-1}$ relative to CAC paste ($4.5 \times 10^{-6}$ °C$^{-1}$). Out of the 3 nanoparticles investigated, NZ resulted in the lowest value of the coefficient of thermal expansion for temperatures between 100 and 900 °C.

## 5.6 Effect of graphite powder

Guo et al. [97] studied the thermal properties of CAC concretes containing various amounts of graphite powder. The mixes included basalt and bauxite aggregate as well as steel fibres with silica and aluminium micro powder. After oven drying at 100 °C for 3 days to remove moisture, the control mix without graphite had a thermal conductivity measured at room temperature of approximately 1.2 W m$^{-1}$ K$^{-1}$. With the addition of 5% graphite powder, the thermal conductivity almost doubled to 2.34 W m$^{-1}$ K$^{-1}$ and it increased

with increasing conditioning temperature up to a value of 2.9 W m$^{-1}$ K$^{-1}$ at 900 °C. On the contrary, the addition of graphite decreased density and compressive strength approximately from 2.86 g cm$^{-3}$ to 2.68 g cm$^{-3}$ and from 54 to 27.2 MPa, respectively. Conditioning at elevated temperatures caused the compressive strength to increase for all temperatures except for 700 °C where the compressive strength decreased to approximately 25 MPa. The shrinkage rate for conditioning temperatures below 700 °C was below 0.2%, while it increased to 1% for temperatures between 900 and 1100 °C.

## 5.7 Effect of metallic additions

Girardi et al. [57] studied the effect of various types of steel fibres, metallic powders and recycled metallic shavings on the thermal properties of PC concrete. The metallic powder was composed of tool steel and had a mean size of 12 μm. The recycled metallic shavings were from rail steel and were 10 mm to 20 mm in length. The thermal conductivity was measured at 25 °C both before and after thermal conditioning at 300 °C for 4 h. The results in Table 4 show that the metallic additions almost double the thermal conductivity compared to the control mix, with the shavings giving the best results. All mixes experienced a decrease in the thermal conductivity after thermal conditioning that is attributed to the loss of water and microcracking. The specific heat was measured using two thermal scans up to 350 °C. During the first scan, all of the mixes showed the expected peak around 100 °C. For the second scan, the mixes with the metallic additions had lower specific heat values than the control mix up until a temperature of

**Table 4** Thermal conductivity with metallic additions [57]

| Additions | Thermal conductivity (W m$^{-1}$ K$^{-1}$) Before thermal conditioning | Thermal conductivity (W m$^{-1}$ K$^{-1}$) After thermal conditioning |
|---|---|---|
| None | 1.02 | 0.99 |
| Steel fibres | 2.01 | 1.73 |
| Nylon fibre and metallic powder | 2.21 | 2.01 |
| Nylon fibres and recycled metallic shavings | 2.74 | 2.13 |

approximately 200 °C, where the values were relatively the same. It was also demonstrated that the different metallic additions do not have any appreciable effect on the coefficient of thermal expansion of concrete.

### 5.8 Prototypes and available products

Most solid block storage systems are based on concrete and research on these materials aims at increasing the temperatures to which they can be subjected. It is possible to prevent crack formation with the addition of fibres [57, 75, 95, 98], the use of geopolymers [99], or the use of calcium aluminate cement, allowing to obtain concretes that can withstand up to 650 °C without cracking [100].

Other similar prototypes, at different scales, are studied in the literature. For example, Skinner et al. [101] present a prototype thermal storage system based on ultra-high-performance concrete with molten salts as heat transfer fluid. The objective of the study was to ensure the durability of the concrete, in particular, that no cracks appeared due to temperature cycles. The materials were tested at temperatures of 400 to 500 °C and the addition of polytetrafluoroethylene (i.e., Teflon) or high temperature fibrous paste and aluminium at the interface between the concrete and the heat exchanger was found to reduce the number and size of cracks.

Different methods, such as modular blocks, can be designed with this type of material. For example, Laing et al. [102] present heat storage blocks that can be combined to adjust the storage capacity, in order to store solar energy. The performance of the prototype has been validated experimentally, considering temperatures between 200 and 400 °C, with a capacity of 1100 MWh.

Another promising way is a modular design using individual thermal elements consisting of encased cylinders filled with concrete like heat storage medium named HEATCRETE® with integrated tubular heat exchangers [103]. These elements can be arranged in series and parallel in the module frame and multiple modules can be hydraulically connected to form thermal batteries. Temperatures up to 380 °C were reached for a prototype having a capacity of $2 \times 500$ kWh (Fig. 9).

A prototype concrete column was also experimentally tested at lower temperatures (about 160 °C) for use in building heating [104]. The concrete column was moulded around a metal pipe and hot air was used to load the column to demonstrate the feasibility and validate a numerical model. This model was then used to simulate temperatures above 300 °C. Laboratory scale prototypes using cast steel and concrete



**Fig. 9** Photograph of fully commissioned EnergyNest thermal energy storage with $4 \times 250$ kWh$_{th}$ capacity at Masdar Institute Solar Platform, United Arab Emirates [103]

as storage material were studied by Rao et al. [105] Although the experimental setup and the prototypes were designed to operate at up to 400 °C, the maximum temperature was limited to 250 °C for charging experiments and 180 °C for thermal cycling due to safety issues. As expected, charging and discharging times were much shorter in the prototype made of cast iron due to the higher thermal conductivity of the material.

Concrete is also widely used for packed bed storage systems and the same issues are addressed (mechanical performance losses). Thermocline system performs better with the use of a fixed bed, compared to a simple structural concrete, in particular with the increase of the storage system dimension [106, 107]. The work of Wu et al. shows that the use of concrete particles in packed beds improves the thermocline effect by reducing the thickness of the thermal gradient [107]. The work of John et al. [5] presents different samples, immersed in a molten salt bath and subjected to high temperatures (300–600 °C) and shows a reduction in the mechanical performance. The authors recommend bricks and concrete slabs based on Portland cement and fly ash in thermocline energy storage systems because they are inexpensive and have good thermal properties. Moreover, the thermal conditioning of concrete and the addition of cementitious materials improve its refractoriness. In the case of Kunwar et al.'s work [108], they use cylindrical drilled concrete blocks (Fig. 10). They point out that increasing the number of holes and their diameter improves the charging time. The tested temperatures are around 300 °C, for a storage capacity of about 5 MJ. A summary of the different materials and means employed are presented in Table 5.

## 6 Concluding remarks

This paper deals with sensitive heat storage using concrete as sensible energy storage medium. Although the energy storage capacity of concrete has certain impact in low temperature applications like housing, most research works are focused in the much higher temperature range relevant for the energy sector. Therefore, characterisation and evaluation methods for determining material performance in such temperature range have been presented and the following conclusions can be drawn.

For thermal properties, thermal conductivity and heat capacity are important to consider. Thermal conductivity and the parameters that influence it have been examined. Due to the many variables, the determination of thermal conductivity must be carried out with care and each test, whether a steady state technique (such as the guarded hot plate and/or heat flow meter method) or a transient approach (the hot wire/hot strip and/or transient plane source method), must be adopted with great care. Results are specific to the test and comparisons with other configurations and materials should be made with caution. Two main techniques are used to determine heat capacity: differential scanning calorimetry and the drop method. The former is the most widely used. The coefficient of thermal expansion and shrinkage are related parameters.



**Fig. 10** Concrete blocks, with different numbers and sizes of holes, used in packed bed solutions for TES [108]

**Table 5** Materials and means employed for different energy sources

| Energy source | Temperatures/power or capacity* | Pro/cons | Materials and means |
|---|---|---|---|
| Solar | 5–1500 °C<br>40–19000 MWh (annual) | Pros:<br>● High potential<br>● High temperature<br>Cons:<br>● Feasibility at high temperature<br>● High costs<br>● Intermittent | Materials:<br>● HTF and solid blocks (concrete, rock, sands)<br>● Molten salts<br>Means:<br>● Parabolic trough collectors<br>● Solar power towers<br>● Linear Fresnel reflectors<br>● Parabolic dish collectors<br>● Adsorption chiller |
| Waste heat recovery | 230–650 °C<br>90,000 MWh (annual) | Pros:<br>● Local usage possible (heating)<br>Cons:<br>● Supplementary infrastructure required after construction of the industry | Materials:<br>● HTF<br>● Molten salts<br>Means:<br>● Adsorption chiller |

*From [7, 102, 103, 109]

High temperatures and temperature cycles can cause the concrete to deteriorate and the thermal conductivity to decrease. The durability of the concrete storage medium is therefore an important parameter to consider. As part of the durability tests, it is necessary to determine the material's susceptibility to limited thermal deformation and the risk of cracking, the coefficient of thermal expansion, etc. Thermal fatigue is tested by imposing variable temperature cycles and can be linked to spalling.

The environmental footprint, as with all construction materials and techniques, can be determined using a variety of software tools. This Life Cycle Assessment (LCA) approach is essential for determining the ecological impact of the material or product under consideration. Sustainability is and will be a major parameter to be discussed, alongside the overall cost of the product and/or material.

Some influencing parameters and results are then presented. The type of cement and the hydrates formed determine the densification of the cement matrix. Thermal properties are linked to temperature during hydration and significant differences up to no effect are reported in the literature. The alternatives to Portland cement (PC) systems, calcium aluminate cement (CAC) composites, alkali activated cement (AAC) composites and hybrid cement (HC) composites containing Portland cement and aluminosilicate precursors, have demonstrated their potential to function as TES systems because they have higher thermal conductivities than Portland cement systems.

The effects of water-cement ratio, (recycled) aggregates, (short) polymer fibres, nanoparticles and other additions were also examined. The results show that conductivity increases as the water-cement ratio decreases. In addition, any difference in the values of the coefficient of thermal expansion between (recycled) aggregates and cement paste must be taken into account. Adding short polypropylene (PP) fibres to the mix reduces the tendency of concrete to spall at high temperatures. Nanoparticles such as nano-silica (NS), nano-magnesia (NM) and nano-zirconia (NZ) appear to improve thermal properties. Thermal conductivity can be increased by adding graphite powder and metallic additions such as fibres, metallic powder and recycled metallic shavings.

In the final section of this paper, the prototypes and products available, with their positive and negative aspects, are examined. There is a plethora of TES applications. In addition to civil engineering applications, stored sensible heat can also be used in the chemical, materials manufacturing, paper and textile industries, among others. It is a promising technology with a high potential to be used in conjunction with renewable energies as an alternative to fossil fuel-based energy solutions.

**Declarations**

**Conflict of interest** The authors declare no conflict of interest.

# References

1. Abdin Z, Khalilpour KR (2019) Single and polystorage technologies for renewable-based hybrid energy systems. Polygeneration with polystorage for chemical and energy hubs. Elsevier, The Netherlands, pp 77–131

2. Ebrahimi M, Keshavarz A (2015) CCHP thermal energy storage. Combined cooling, heating and power. Elsevier, The Netherlands, pp 183–188

3. Hussain F, Rahman MZ, Sivasengaran AN, Hasanuzzaman M (2020) Energy storage technologies. Energy for sustainable development. Elsevier, The Netherlands, pp 125–165

4. Wang RZ, Xu ZY, Ge TS (2016) Introduction to solar heating and cooling systems. Advances in solar heating and cooling. Elsevier, The Netherlands, pp 3–12

5. John E, Hale M, Selvam P (2013) Concrete as a thermal energy storage medium for thermocline solar energy storage systems. Sol Energy 96:194–204. https://doi.org/10.1016/j.solener.2013.06.033

6. Kuznik F, Opel O, Osterland T, Ruck WKL (2021) Thermal energy storage for space heating and domestic hot water in individual residential buildings. Advances in thermal energy storage systems. Elsevier, The Netherlands, pp 567–594

7. Alva G, Lin Y, Fang G (2018) An overview of thermal energy storage systems. Energy 144:341–378. https://doi.org/10.1016/j.energy.2017.12.037

8. Imessad K, Derradji L, Messaoudene NA et al (2014) Impact of passive cooling techniques on energy demand for residential buildings in a Mediterranean climate. Renew Energy 71:589–597. https://doi.org/10.1016/j.renene.2014.06.005

9. Miró L, Navarro ME, Suresh P et al (2014) Experimental characterization of a solid industrial by-product as material for high temperature sensible thermal energy storage (TES). Appl Energy 113:1261–1268. https://doi.org/10.1016/j.apenergy.2013.08.082

10. Kumar A, Kishore VVN (1999) Construction and operational experience of a 6000 $m^2$ solar pond at Kutch, India. Sol Energy 65:237–249. https://doi.org/10.1016/s0038-092x(98)00134-0

11. Jiménez-Arreola M, Pili R, Magro FD et al (2018) Thermal power fluctuations in waste heat to power systems: an overview on the challenges and current solutions. Appl Therm Eng 134:576–584. https://doi.org/10.1016/j.applthermaleng.2018.02.033

12. Kumar L, Hasanuzzaman M, Rahim NA (2019) Global advancement of solar thermal energy technologies for industrial process heat and its future prospects: a review. Energy Convers Manag 195:885–908. https://doi.org/10.1016/j.enconman.2019.05.081

13. Kalogirou SA (2004) Solar thermal collectors and applications. Prog Energy Combust Sci 30:231–295. https://doi.org/10.1016/j.pecs.2004.02.001

14. Wang H, Hua P, Wu X et al (2022) Heat-power decoupling and energy saving of the CHP unit with heat pump based waste heat recovery system. Energy 250:123846. https://doi.org/10.1016/j.energy.2022.123846

15. Laing D, Steinmann W-D, Tamme R (2008) Sensible Heat Storage for Medium and High Temperatures. In: Proceedings of ISES World Congress 2007 (Vol. I–V). Springer Berlin Heidelberg, pp 2731–2735

16. Mohan G, Venkataraman MB, Coventry J (2019) Sensible energy storage options for concentrating solar power plants operating above 600 °C. Renew Susin Energy Rev 107:319–337. https://doi.org/10.1016/j.rser.2019.01.062

17. González-Roubaud E, Pérez-Osorio D, Prieto C (2017) Review of commercial thermal energy storage in concentrated solar power plants: Steam vs. molten salts. Renew Sustain Energy Rev 80:133–148. https://doi.org/10.1016/j.rser.2017.05.084

18. Salomoni VA, Majorana CE, Giannuzzi GM et al (2014) Thermal storage of sensible heat using concrete modules in solar power plants. Sol Energy 103:303–315. https://doi.org/10.1016/j.solener.2014.02.022

19. Pimienta P, McNamee RJ, Mindeguia J-C (2019) Physical Properties and Behaviour of High-Performance Concrete at High Temperature. Springer International Publishing, Cham

20. Asadi I, Shafigh P, Hassan ZFBA, Mahyuddin NB (2018) Thermal conductivity of concrete—a review. J Build Eng 20:81–93. https://doi.org/10.1016/j.jobe.2018.07.002

21. Ndiaye K, Ginestet S, Cyr M (2018) Thermal energy storage based on cementitious materials: a review. AIMS Energy 6:97–120. https://doi.org/10.3934/energy.2018.1.97

22. Samson G, Phelipot-Mardelé A, Lanos C (2017) A review of thermomechanical properties of lightweight concrete. Mag Concr Res 69:201–216. https://doi.org/10.1680/jmacr.16.00324

23. Navarro ME, Martinez M, Gil A et al (2012) Selection and characterization of recycled materials for sensible thermal energy storage. Sol Energy Mater Sol Cells 107:131–135. https://doi.org/10.1016/j.solmat.2012.07.032

24. Fernandez AI, Martinez M, Segarra M et al (2010) Selection of materials with potential in sensible thermal energy storage. Sol Energy Mater Sol Cells 94:1723–1729. https://doi.org/10.1016/j.solmat.2010.05.035

25. Khare S, DelltextquotesingleAmico M, Knight C, McGarry S (2013) Selection of materials for high temperature sensible energy storage. Sol Energy Mater Sol Cells 115:114–122. https://doi.org/10.1016/j.solmat.2013.03.009

26. Eurocode 2 (2004) Design of concrete structures - Part 1–1: General rules and rules for buildings. European Committee for Standardization

27. Palacios A, Cong L, Navarro ME et al (2019) Thermal conductivity measurement techniques for characterizing thermal energy storage materials—a review. Renew Sustain Energy Rev 108:32–52. https://doi.org/10.1016/j.rser.2019.03.020

28. Buck W, Rudtsch S (2006) Thermal properties. Springer handbook of materials measurement methods. Springer, Berlin Heidelberg, pp 399–429

29. Lele AF, NtextquotesingleTsoukpoe KE, Osterland T et al (2015) Thermal conductivity measurement of thermochemical storage materials. Appl Therm Eng 89:916–926. https://doi.org/10.1016/j.applthermaleng.2015.06.077

30. Salmon D (2001) Thermal conductivity of insulations using guarded hot plates, including recent developments and sources of reference materials. Meas Sci Technol 12:R89–R98. https://doi.org/10.1088/0957-0233/12/12/201

31. Rouhani M, Huttema W, Bahrami M (2018) Effective thermal conductivity of packed bed adsorbers: part 1—experimental study. Int J Heat Mass Transf 123:1204–1211. https://doi.org/10.1016/j.ijheatmasstransfer.2018.01.142

32. Kim S, Drzal LT (2009) High latent heat storage and high thermal conductive phase change materials using exfoliated graphite nanoplatelets. Sol Energy Mater Sol Cells 93:136–142. https://doi.org/10.1016/j.solmat.2008.09.010

33. Fabiani C, Pisello AL (2018) Coupling the transient plane source method with a dynamically controlled environment to study PCM-doped building materials. Energy Build 180:122–134. https://doi.org/10.1016/j.enbuild.2018.09.008

34. Johansson P, Adl-Zarrabi B, Hagentoft C-E (2012) Using transient plane source sensor for determination of thermal properties of vacuum insulation panels. Front Archit Res 1:334–340. https://doi.org/10.1016/j.foar.2012.09.004

35. Gustafsson SE (1991) Transient plane source techniques for thermal conductivity and thermal diffusivity measurements of solid materials. Rev Sci Instrum 62:797–804. https://doi.org/10.1063/1.1142087

36. Pei G, Xiang J, Li G et al (2019) A literature review of heat capacity measurement methods. The minerals, metals & materials series. Springer International Publishing, Cham, pp 569–577

37. Razouk R, Beaumont O, Hameury J, Hay B (2021) Towards accurate measurements of specific heat of solids by drop calorimetry up to 3000 °C. Thermal Science and Engineering Progress 26:101130. https://doi.org/10.1016/j.tsep.2021.101130

38. Flammersheim HJ, Hemminger WF, Höhne G (2003) Differential scanning calorimetry. Springer, Berlin Heidelberg

39. Rolka P, Przybylinski T, Kwidzinski R, Lackowski M (2021) The heat capacity of low-temperature phase change materials (PCM) applied in thermal energy storage systems. Renew Energy 172:541–550. https://doi.org/10.1016/j.renene.2021.03.038

40. Ferrer G, Barreneche C, Solé A et al (2017) New proposed methodology for specific heat capacity determination of materials for thermal energy storage (TES) by DSC. J Energy 11:1–6. https://doi.org/10.1016/j.est.2017.02.002

41. Ramachandran VS, Beaudoin JJ (2001) Handbook of analytic techniques in concrete science and technology (building materials series). Noyes Publications, New York

42. Suryanarayana C, Norton MG (1998) X-ray diffraction a practical approach. Springer, US

43. Taylor HFW (1997) Cement chemistry. T. Telford, Shropshire

44. Bezerra UT, Martinelli AE, Melo DMA et al (2011) The strength retrogression of special class Portland oilwell cement. Cerâmica 57:150–154. https://doi.org/10.1590/s0366-69132011000200004

45. Sabeur H, Platret G, Vincent J (2016) Composition and microstructural changes in an aged cement pastes upon two heating–cooling regimes, as studied by thermal analysis and X-ray diffraction. J Therm Anal Calorim 126:1023–1043. https://doi.org/10.1007/s10973-016-5639-8

46. Piasta J, Sawicz Z, Rudzinski L (1984) Changes in the structure of hardened cement paste due to high temperature. Matériaux et Constr 17:291–296. https://doi.org/10.1007/bf02479085

47. Ebnesajjad C (2013) Surface Treatment of Materials for Adhesive Bonding. William Andrew Inc

48. Colpan CO, Nalbant Y, Ercelik M (2018) 4.28 Fundamentals of fuel cell technologies. Comprehensive energy systems. Elsevier, The Netherlands, pp 1107–1130

49. Fernández ÁG, Boquera L, Cabeza LF (2018) characterization of materials for sensible thermal energy storage at high temperature. Recent advancements in materials and systems for thermal energy storage. Springer International Publishing, Cham, pp 69–88

50. Wunderlich B (2001) Encyclopedia of materials: science and technology. Elsevier, Oxford, pp 9134–9141

51. Dannemand M, Delgado M, Lazaro A et al (2018) Porosity and density measurements of sodium acetate trihydrate for thermal energy storage. Appl Therm Eng 131:707–714. https://doi.org/10.1016/j.applthermaleng.2017.12.052

52. de Terris T, Andreau O, Peyre P et al (2019) Optimization and comparison of porosity rate measurement methods of selective laser melted metallic parts. Addit Manuf 28:802–813. https://doi.org/10.1016/j.addma.2019.05.035

53. Nasrollahzadeh M, Atarod M, Sajjadi M, et al. (2019) Plant-Mediated Green Synthesis of Nanostructures: Mechanisms, Characterization, and Applications. In: Interface Science and Technology. Elsevier, pp 199–322

54. Diamond S (2007) Durability of Concrete and Cement Composites. In: Page CL, Page MM (eds). Woodhead Publishing, pp 10–44

55. Sogbossi H, Verdier J, Multon S (2019) New approach for the measurement of gas permeability and porosity accessible to gas in vacuum and under pressure. Cement Concr Compos 103:59–70. https://doi.org/10.1016/j.cemconcomp.2019.04.032

56. Gaitero JJ, Campillo I, Guerrero A (2008) Reduction of the calcium leaching rate of cement paste by addition of silica nanoparticles. Cem Concr Res 38:1112–1118. https://doi.org/10.1016/j.cemconres.2008.03.021

57. Roig-Flores M, Lucio-Martin T, Alonso MC, Guerreiro L (2021) Evolution of thermo-mechanical properties of concrete with calcium aluminate cement and special aggregates for energy storage. Cem Concr Res 141:106323. https://doi.org/10.1016/j.cemconres.2020.106323

58. Girardi F, Giannuzzi GM, Mazzei D et al (2017) Recycled additions for improving the thermal conductivity of concrete in preparing energy storage systems. Constr Build Mater 135:565–579. https://doi.org/10.1016/j.conbuildmat.2016.12.179

59. Bergstrom JS (2015) Mechanics of Solid Polymers: Theory and Computational Modeling. William Andrew Inc

60. Diamond S (2004) Special issue on scanning electron microscopy of cements and concretes. Cement Concr Compos 26:917–918. https://doi.org/10.1016/j.cemconcomp.2004.02.027

61. Alarcon-Ruiz L, Platret G, Massieu E, Ehrlacher A (2005) The use of thermal analysis in assessing the effect of temperature on a cement paste. Cem Concr Res 35:609–613. https://doi.org/10.1016/j.cemconres.2004.06.015

62. Torres-Carrasco M, del Campo A, de la Rubia MA et al (2017) New insights in weathering analysis of anhydrous cements by using high spectral and spatial resolution confocal Raman Microscopy. Cem Concr Res 100:119–128. https://doi.org/10.1016/j.cemconres.2017.06.003

63. Torres-Carrasco M, Campo A, Rubia MA et al (2019) In situ full view of the Portland cement hydration by confocal Raman microscopy. J Raman Spectrosc 50:720–730. https://doi.org/10.1002/jrs.5574

64. John EE, Hale WM, Selvam RP (2011) Development of a High-Performance Concrete to Store Thermal Energy for Concentrating Solar Power Plants. In: ASME 2011 5th International Conference on Energy Sustainability, Parts A, B, and C. ASMEDC

65. Lucio-Martin T, Roig-Flores M, Izquierdo M, Alonso MC (2021) Thermal conductivity of concrete at high temperatures for thermal energy storage applications: Experimental analysis. Sol Energy 214:430–442. https://doi.org/10.1016/j.solener.2020.12.005

66. Kannangara T, Joseph P, Fragomeni S, Guerrieri M (2022) Existing theories of concrete spalling and test methods relating to moisture migration patterns upon exposure to elevated temperatures—a review. Case Stud Constr Mater 16:e01111. https://doi.org/10.1016/j.cscm.2022.e01111

67. Suescum-Morales D, Ros JD, Concha AM-DL et al (2021) Effect of moderate temperatures on compressive strength of ultra-high-performance concrete: a microstructural analysis. Cem Concr Res 140:106303. https://doi.org/10.1016/j.cemconres.2020.106303

68. Ma Q, Guo R, Zhao Z et al (2015) Mechanical properties of concrete at high temperature—a review. Constr Build Mater 93:371–383. https://doi.org/10.1016/j.conbuildmat.2015.05.131

69. Zeng H, Li W, Jin M et al (2022) Deterioration of performances and structures of cement pastes under the action of thermal cycling fatigue. Int J Fatigue 165:107181. https://doi.org/10.1016/j.ijfatigue.2022.107181

70. Batuecas E, Ramón-Álvarez I, Sánchez-Delgado S, Torres-Carrasco M (2021) Carbon footprint and water use of alkali-activated and hybrid cement mortars. J Clean Prod 319:128653. https://doi.org/10.1016/j.jclepro.2021.128653

71. Ramón-Álvarez I, Batuecas E, Sánchez-Delgado S, Torres-Carrasco M (2023) Mechanical performance after high-temperature exposure and Life Cycle Assessment (LCA) according to unit of stored energy of alternative mortars to Portland cement. Constr Build Mater 365:130082. https://doi.org/10.1016/j.conbuildmat.2022.130082

72. Laing D, Steinmann WD, Viebahn P et al (2010) Economic analysis and life cycle assessment of concrete thermal energy storage for parabolic trough power plants. J Sol Energy Eng. https://doi.org/10.1115/1.4001404

73. Miró L, Oró E, Boer D, Cabeza LF (2015) Embodied energy in thermal energy storage (TES) systems for high temperature applications. Appl Energy 137:793–799. https://doi.org/10.1016/j.apenergy.2014.06.062

74. Selvam RP, Hale M, Strasser M (2013) Development and Performance Evaluation of High Temperature Concrete for Thermal Energy Storage for Solar Power Generation. Office of Scientific and Technical Information (OSTI)

75. John EE, Hale WM, Selvam RP (2010) Effect of High Temperatures and Heating Rates on High Strength Concrete for Use as Thermal Energy Storage. In: ASME 2010 4th International Conference on Energy Sustainability, Volume 2. ASMEDC

76. Ashby MF (2004) Materials selection in mechanical design. Elsevier Science & Technology Books, The Nertherlands

77. Ashby M (2007) Materials engineering, science, processing and design. Elsevier Butterworth-Heinemann, Oxford

78. Khoury GA (1992) Compressive strength of concrete at high temperatures: a reassessment. Mag Concr Res 44:291–309. https://doi.org/10.1680/macr.1992.44.161.291

79. Ukrainczyk N, Matusinovic T (2010) Thermal properties of hydrating calcium aluminate cement pastes. Cem Concr Res 40:128–136. https://doi.org/10.1016/j.cemconres.2009.09.005

80. Alonso MC, Vera-Agullo J, Guerreiro L et al (2016) Calcium aluminate based cement for concrete to be used as thermal energy storage in solar thermal electricity plants. Cem Concr Res 82:74–86. https://doi.org/10.1016/j.cemconres.2015.12.013

81. dos Santos WN (2003) Effect of moisture and porosity on the thermal properties of a conventional refractory concrete. J Eur Ceram Soc 23:745–755. https://doi.org/10.1016/s0955-2219(02)00158-9

82. Pan J, Zou R, Jin F (2016) Experimental study on specific heat of concrete at high temperatures and its influence on thermal energy storage. Energies 10:33. https://doi.org/10.3390/en10010033

83. Ramón-Álvarez I, Marugán-Cruz C, Enrquez E et al (2023) Alkali-activated and hybrid materials: Alternative to Portland cement as a storage media for solar thermal energy. Boletin de la Sociedad Española de Cerámica y Vidrio 62:160–173. https://doi.org/10.1016/j.bsecv.2021.11.006

84. Provis JL, Van Deventer JS (2014) Alkali activated materials: state-of-the-art report, RILEM TC 224-AAM. Springer, Netherlands

85. Amer I, Kohail M, El-Feky MS et al (2021) Characterization of alkali-activated hybrid slag/cement concrete. Ain Shams Eng J 12:135–144. https://doi.org/10.1016/j.asej.2020.08.003

86. Al-Kutti W, Nasir M, Johari MAM et al (2018) An overview and experimental study on hybrid binders containing date palm ash, fly ash, OPC and activator composites. Constr Build Mater 159:567–577. https://doi.org/10.1016/j.conbuildmat.2017.11.017

87. Choubi SS, Akgul CM (2022) High temperature exposure of alkali-activated coal fly ashes. J Build Eng 59:105081. https://doi.org/10.1016/j.jobe.2022.105081

88. Kantarci F, Türkmen I, Ekinci E (2021) Improving elevated temperature performance of geopolymer concrete utilizing nano-silica, micro-silica and styrene-butadiene latex. Constr Build Mater 286:122980. https://doi.org/10.1016/j.conbuildmat.2021.122980

89. Duan P, Yan C, Zhou W et al (2015) An investigation of the microstructure and durability of a fluidized bed fly ash–metakaolin geopolymer after heat and acid exposure. Mater Des 74:125–137. https://doi.org/10.1016/j.matdes.2015.03.009

90. Fu H, Mo R, Wang P et al (2022) Influence of elevated temperatures and cooling method on the microstructure development and phase evolution of alkali-activated slag. Materials 15:2022. https://doi.org/10.3390/ma15062022

91. Fernández-Jiménez A, Garcia-Lodeiro I, Maltseva O, Palomo A (2018) Hydration mechanisms of hybrid cements as a function of the way of addition of chemicals. J Am Ceram Soc 102:427–436. https://doi.org/10.1111/jace.15939

92. Garcia-Lodeiro I, Boudissa N, Fernandez-Jimenez A, Palomo A (2018) Use of clays in alkaline hybrid cement preparation. The role of bentonites Materials Letters 233:134–137. https://doi.org/10.1016/j.matlet.2018.08.098

93. Hochstein DP, Meyer C (2016) Measurement and prediction of thermal conductivity of cement paste. ACI Mater J. https://doi.org/10.14359/51688643

94. Zhang W, Min H, Gu X et al (2015) Mesoscale model for thermal conductivity of concrete. Constr Build Mater 98:8–16. https://doi.org/10.1016/j.conbuildmat.2015.08.106

95. Bentz D, Peltz M, Durán-Herrera A et al (2010) Thermal properties of high-volume fly ash mortars and concretes. J Building Phys 34:263–275. https://doi.org/10.1177/1744259110376613

96. Kodur VKR, Sultan MA (2003) Effect of temperature on thermal properties of high-strength concrete. J Mater Civ Eng 15:101–107. https://doi.org/10.1061/(asce)0899-1561(2003)15:2(101)

97. Ozger OB, Girardi F, Giannuzzi GM et al (2013) Effect of nylon fibres on mechanical and thermal properties of hardened concrete for energy storage systems. Mater Des 51:989–997. https://doi.org/10.1016/j.matdes.2013.04.085

98. Jiang C, Yuan H, Lu C et al (2018) The effect of nanoparticles on the properties of calcium aluminate cement pastes at high temperatures. Adv Cem Res 30:195–203. https://doi.org/10.1680/jadcr.17.00039

99. Guo C, Zhu J, Zhou W, Chen W (2010) Fabrication and thermal properties of a new heat storage concrete material. J Wuhan Univ Technol-Mater Sci Ed 25:628–630. https://doi.org/10.1007/s11595-010-0058-3

100. Boquera L, Pons D, Fernández AI, Cabeza LF (2021) Characterization of supplementary cementitious materials and fibers to be implemented in high temperature concretes for thermal energy storage (TES) application. Energies 14:5190. https://doi.org/10.3390/en14165190

101. Rahjoo M, Goracci G, Martauz P et al (2022) geopolymer concrete performance study for high-temperature thermal energy storage (TES) applications. Sustainability 14:1937. https://doi.org/10.3390/su14031937

102. Boquera L, Castro JR, Pisello AL et al (2022) Thermomechanical stability of supplementary cementitious materials in cement paste to be incorporated in concrete as thermal energy storage material at high temperatures. J Energy Storage 54:105370. https://doi.org/10.1016/j.est.2022.105370

103. Skinner JE, Brown BM, Selvam RP (2011) Testing of high performance concrete as a thermal energy storage medium at high temperatures. In: ASME 2011 5th international conference on energy sustainability, parts A, B, and C. ASMEDC

104. Laing D, Bahl C, Bauer T et al (2012) High-temperature solid-media thermal energy storage for solar thermal power plants. Proc IEEE 100:516–524. https://doi.org/10.1109/jproc.2011.2154290

105. Hoivik N, Greiner C, Barragan J et al (2019) Long-term performance results of concrete-based modular thermal energy storage system. J Energy Storage 24:100735. https://doi.org/10.1016/j.est.2019.04.009

106. Özrahat E, Ünalan S (2017) Thermal performance of a concrete column as a sensible thermal energy storage medium and a heater. Renew Energy 111:561–579. https://doi.org/10.1016/j.renene.2017.04.046

107. Rao CRC, Niyas H, Muthukumar P (2018) Performance tests on lab-scale sensible heat storage prototypes. Appl Therm Eng 129:953–967. https://doi.org/10.1016/j.applthermaleng.2017.10.085

108. Strasser MN, Selvam RP (2014) A cost and performance comparison of packed bed and structured thermocline thermal energy storage systems. Sol Energy 108:390–402. https://doi.org/10.1016/j.solener.2014.07.023

109. Wu M, Li M, Xu C et al (2014) The impact of concrete structure on the thermal performance of the dual-media thermocline thermal storage tank using concrete as the solid medium. Appl Energy 113:1363–1371. https://doi.org/10.1016/j.apenergy.2013.08.044

110. Kunwar A, Kumar M, Gupta A et al (2019) Experimental investigation of a packed-bed thermal energy storage system fitted with perforated cylindrical elements. Heat Mass Transf 55:2723–2737. https://doi.org/10.1007/s00231-019-02609-x

111. Loni R, Najafi G, Bellos E et al (2021) A review of industrial waste heat recovery system for power generation with organic rankine cycle: recent challenges and future outlook. J Clean Prod 287:125070. https://doi.org/10.1016/j.jclepro.2020.125070